Range Extension Control System for Electric Vehicles Based on Front and Rear Driving Force Distribution Considering Load Transfer

Sho Egami and Hiroshi Fujimoto
The University of Tokyo
5-1-5, Kashiwanoha, Kashiwa, Chiba, 227-8561 Japan
Phone: +81-4-7136-4131
Fax: +81-4-7136-4132
Email: egami@fujilab.k.u-tokyo.ac.jp, fujimoto@k.u-tokyo.ac.jp

***Abstract*—Electric vehicles (EVs) are more highly efficient than internal combustion engine vehicles. However, EVs have a disadvantage in that the mileage per charge is short. In this paper, a range extension control system (RECS) based on a load transfer is proposed. The minimum acceleration resistance can be realized through driving force distribution ratio between front and rear wheels. Therefore, the proposed RECS fulfills maximum efficiency. Simulations and experiments are carried out to confirm the effectiveness of the proposed system.**

I. Introduction

Recently, electric vehicles (EVs) are actively researched in order to solve environmental problems and fossil fuel shortage. Hybrid vehicles (HEVs) and EVs have already been marketed and they are more ecological than the internal combustion engine vehicles (ICEVs). In addition to this ecological merit, EVs have the following advantages from the view point of vehicle motion control.

- In-wheel motors can be attached to each wheel and enables independent control of each wheel.
- Regeneration barke is available.
- Generated torque can be measured precisely from motor current.
- Torque response is fast.

By making use of these advantages, the advanced vehicle motion control can be achieved [1], [2]. From this point of view, our research group has proposed many motion control methods for EVs [3], [4].

The electric motor, which is the power source of EVs, is much more efficient than internal combustion engine. However, the energy density of battery that is the energy source of EVs is only one tenth of the oil fuel. Therefore, the mileage per charge is short in EVs. This is a critical issue for widely use of EVs. Hence, in this paper, the range extension control system (RECS) based on a load transfer of vehicle is proposed. This method can be used when the electric vehicle keeps an acceleration. The conventional vehicle system distributes a torque in specific ratio of the front and rear wheels as FWD, RWD, or 4WD. The proposed method minimizes the motor output by distributing the optimum driving force of front and rear wheels based on load transfer consideration.

When the vehicle keeps an acceleration, a component of normal force of vehicle is biased from front wheel to rear wheel by the inertia force acting on the chassis. The driving force is a product of the road friction and the normal force on tire. The road friction depends on the slip ratio. Therefore, the slip ratio required for a certain driving force varies when the normal force is biased. In this method, the optimum driving force distribution control considering normal force in front and rear wheels is proposed. The optimum distribution ratio is derived. It is effective for the extension of the miles per charge so that the energy required for the acceleration can be decreased. Simulations and experiments are carried out to confirm the effectiveness of the proposed method.

In this paper, the optimization method from the motor output to the vehicle driving force is examined. In addition to this method, our research group also studies the optimization method from the motor output to translational speed and yaw-rate [5], or from the electric source to the motor output considering the electric loss [6].

II. Experiment vehicle

The electric vehicle “FPEV2-Kanon” developed by authors’s laboratory was used for experiments. The outer-rotor type in-wheel motors produced by TOYO DENKI SEIZO K.K. are installed as driving powertrain in each wheel. Since these in-wheel motors are direct drive system, the backlash of reduction gear does not influence the control performance. These motors can be independently driven by inverters. Fig. 1 shows FPEV2-Kanon and in-wheel motors. Table. I shows the specification of FPEV2-Kanon. In the proposed method, it is assumed that left and right wheels generate the same driving forces. Therefore, it is applicable in not only a vehicle which each wheel independently can be driven but also a vehicle installed multiple power source for front and rear wheel.

(a) FPEV2-Kanon

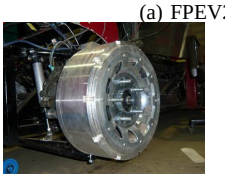

(b) Front Motor

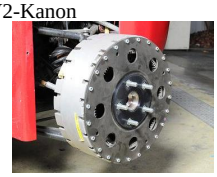

(c) Rear Motor

Fig. 1. Experimental vehicle

TABLE I
VEHICLE PARAMETER

Vehicle Mass M_0	854 kg
Wheelbase l	1715 mm
Distance from center of gravity to front/rear axle tread l_f,l_r	Front: 1013 mm
	Rear: 702 mm
Gravity height h_g	0.51 m
Wheel Inertia J_{wf}	1.24 Nms^2
Wheel Inertia J_{wr}	1.26 Nms^2
Wheel Radius r	0.302 m

III. VEHICLE MODELING

A. Longitudial vehicle model

In this subsection, the vehicle model for driving force control is explained. Using one wheel model and bicycle model as shown in Fig. 2, Fig. 3, the equations both of the wheel and the vehicle in longitudinal vehicle motion can be represented by

$$J_{wi}\dot{\omega}_i = T_i - rF_{di}, \quad (1)$$
$$M\dot{V} = F_{ref}, \quad (2)$$
$$V_{wi} = r\omega_i, \quad (3)$$

where ω_i[rad/s] is the wheel angular velocity, V[m/s] is the vehicle velocity, V_{wi}[m/s] is the wheel velocity, T_i[Nm] is the motor torque, F_{di}[N] is the driving force, M[kg] is the mass of bicycle model, r[m] is the wheel radius, and J_{wi}[Nms^2] is the wheel inertia. The subscript i is inserted the character f or r that means front or rear wheel. The mass of bicycle model is defined as

$$M = \frac{M_0}{2}, \quad (4)$$

where M_0 is the vehicle mass. In the right and left wheels, the same controller is implemented in order to make zero yaw moment. The vehicle driving force, shown in Fig. 3, is total driving force of front and rear wheels.

$$F_{ref} = F_{df} + F_{dr} \quad (5)$$

The slip ratio is defined as

$$\lambda_i = \frac{V_{wi} - V}{\max(V_{wi}, V, \epsilon)}, \quad (6)$$

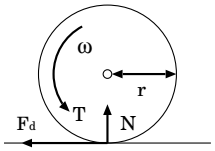

Fig. 2. Wheel Model

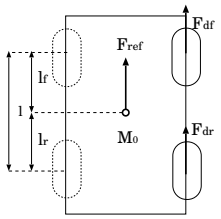

Fig. 3. Bicycle Model

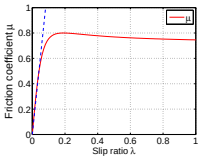

Fig. 4. Friction Curve

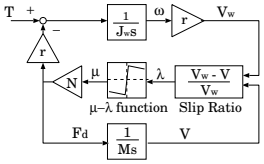

Fig. 5. Vehicle Model Diagram

where $\epsilon \ll 1$ is the small constant value to avoid zero denominator. The sign of difference between V_{wi} and V is changed in powering operation and regeneration. In this paper, $\max(V_{wi}, V, \epsilon) = V_{wi}$ is given all time because we consider acceleration only. The slip ratio λ_i is represented by

$$\lambda_i = \frac{V_{wi} - V}{V_{wi}}. \quad (7)$$

The friction coefficient μ_i is a function of the slip ratio λ_i. In the simulation, Magic Formula is adopted as the model of friction cofficient curve [7]. The driving force F_{di} is represented as

$$F_{di} = \mu_i N_i, \quad (8)$$

where N_i is the normal force. The drving force is also defined as

$$F_{di} = D_{si}\lambda_i, \quad (9)$$
$$= D'_s N_i \lambda_i, \quad (10)$$

where D_{si} is the driving stiffness. In Fig. 4, when the slip ratio λ_i is small, the friction coefficient μ_i is linearly proportional to the slip ratio λ_i. In this paper, it is assumed that the slip ratio is small because of the high friction road. Therefore, the coefficient D'_s is constant. Coefficient D'_s depend on a condition of road, and represented by

$$D'_s = \frac{\partial \mu}{\partial \lambda} |_{\lambda=0}. \quad (11)$$

B. Normal force model

In this subsection, the influence of load transfer caused by longitudinal acceleration is explained. When the vehicle accelerates, the load transfer of normal force influences the driving force for a unit slip ratio. The normal force in front and rear wheels considering a longitudinal acceleration is given as

$$N_f = \frac{l_r}{l} Mg - a_x M \frac{h_g}{l}, \quad (12)$$
$$N_r = \frac{l_f}{l} Mg + a_x M \frac{h_g}{l}, \quad (13)$$

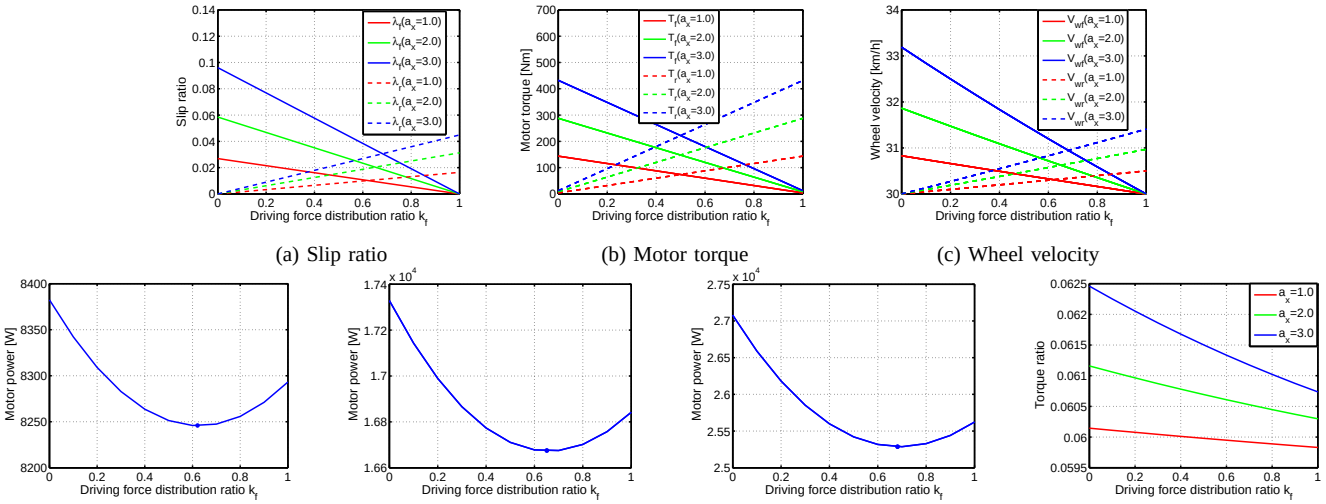

(a) Slip ratio (b) Motor torque (c) Wheel velocity

(d) Total motor output (a_x=1.0) (e) Total motor output (a_x=2.0) (f) Total motor output (a_x=3.0) (g) Torque ratio

Fig. 6. Each Quantity for Driving Force Distribution Ratio

where a_x[m/s^2] is the longitudinal acceleration. Therefore, the driving force of front and rear wheels is described as

$$F_{df} = D_s'(\frac{l_r}{l}Mg - a_x M\frac{h_g}{l})\lambda_f, \tag{14}$$

$$F_{dr} = D_s'(\frac{l_f}{l}Mg + a_x M\frac{h_g}{l})\lambda_r. \tag{15}$$

In front and rear wheels, the driving force for a unit slip ratio is different.

IV. Driving Force Distribution Laws

In this section, total motor output is estimated for front and rear driving force distribution control. The motor power is a product of the motor torque and the wheel angular velocity. Driving force distribution ratio k_f for vehicle driving force is introduced. The driving force in front and rear wheel is defined as

$$F_{dr} = k_f F_{ref}, \tag{16}$$

$$F_{df} = (1-k_f)F_{ref}, \tag{17}$$

$$F_{ref} = F_{df} + F_{dr}. \tag{18}$$

Total motor output changes since a unit slip ratio to driving force for any driving force distribution ratio changes. The equation both of the motor torque and the wheel angular velocity based on slip ratio is represented by

$$T_i = rF_{di} + J_{wi}\dot{\omega}_i, \tag{19}$$

$$\omega_i = \frac{V}{r}\frac{1}{1-\lambda_i}. \tag{20}$$

The motor torque is attributed to the driving force and the rotating inertial force in the wheel. The rotating inertial force is a function of slip ratio, and that equation is represented by

$$J_{wi}\dot{\omega}_i = \frac{J_{wi}}{r}\Big(\frac{a_x}{1-\lambda_i} + \frac{V\dot{\lambda}_i}{(1-\lambda_i)^2}\Big). \tag{21}$$

In this paper, the steady state of driving force is only assumed for the loss evaluation. Therefore the derivative term of slip ratio $\dot{\lambda}_i$ in (21) is ignored.

The motor output and some quantity related to the motor power for driving force were calculated. In this simulation, the vehicle specification, shown in Table. I is used. It is assumed that the vehicle is accelerated by the driving force $F_{ref} = Ma_x$ at 30 [km/h]. The simulation result for modifying the driving force distribution ratio is shown in Fig. 6. Fig. 6(a) shows that the slip ratio to the driving force varies for any distribution ratio due to the influence of normal force on tire. Fig. 6(b) and Fig. 6(c) show that the motor torque is dominated by driving force, and the wheel velocity is relatively infulenced by the slip ratio. It is confirmed that total motor output for specific driving distribution ratio is minimum from Fig. 6(d), Fig. 6(e) and Fig. 6(f). This driving force distribution ratio is the optimum distribution ratio. It is also shown that the optimum distribution ratio changes because the influence of load transfer becomes larger with increasing the acceleration. The propotion of the torque based on the driving force to the inertial torque is defined as

$$T_{ratio} = \frac{J_{wf}\dot{\omega}_f + J_{wr}\dot{\omega}_r}{rF_{df} + rF_{dr}}. \tag{22}$$

From Fig. 6(g), the proportion of the inertial torque is much less than that of the torque based on the driving force.

A. Derivation of the optimum distribution ratio

In this subsection, the derivation of the optimum distribution ratio for the vehicle driving force is explained. The motor torque model, ignored the inertial torque, is given as

$$T_i = rF_{di}. \tag{23}$$

The inertial torque is much less than the torque based on the driving force as shown in Fig. 6(g). Therefore, it is adequate for the derivation of optimum distribution ratio. Total motor

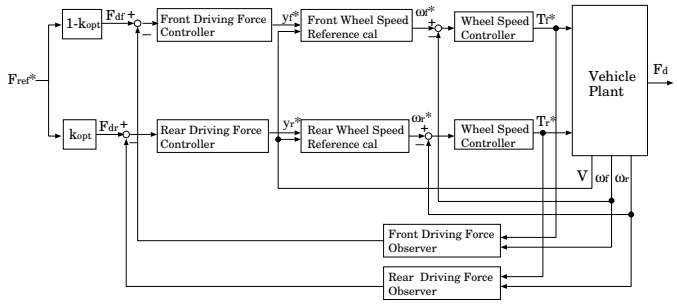

Fig. 7. Optimal Driving Force Distribution Control System

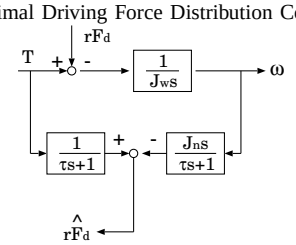

Fig. 8. Driving Force Observer

output is sum of the motor output in front and rear wheels. From motor torque in (23) and wheel angular velocity in (20), the total motor power is represented by

$$\begin{aligned} P_{out} &= P_f + P_r, \\ &= \omega_f T_f + \omega_r T_r, \\ &= V F_{ref}\Big(\frac{1-k_f}{1-\lambda_f} + \frac{k_f}{1-\lambda_r}\Big), \end{aligned} \tag{24}$$

$$\lambda_f = \frac{(1-k_f)F_{ref}}{D_s' N_f}, \tag{25}$$

$$\lambda_r = \frac{k_f F_{ref}}{D_s' N_r}. \tag{26}$$

The optimum driving force ratio is introduced by solving partial differential equation with respect to the distribution ratio k_f. The optimum driving force is represented by

$$k_{opt} = \frac{N_r}{N_r + N_f}. \tag{27}$$

V. Driving force distribution control system

A. The control input of driving force

In this subsection, the control input for driving force is explained. From (9), (10), the slip ratio can be used for the control input of driving force. The slip ratio is inconvenient for control input of the driving force. Thus the control input y_i meaned the relation of the slip ratio is alternatively used. The control input y_i for driving force is represented by

$$y_i = \frac{V_{wi}}{V} - 1. \tag{28}$$

When vehicle accelerates, the control input y_i with respect to the slip ratio λ_i is repsented by

$$y_i = \frac{\lambda_i}{1-\lambda_i}. \tag{29}$$

A quantity of control input y_i is the almost the same as that of slip ratio in the vicinity of $\lambda_i = 0$. Moreover the slip ratio is very small since the tire is adhesive. Therefore, in this peper, it is assumed that the the control input y_i is equal to the slip ratio λ_i. From (28), the wheel velocity reference is represented by

$$V_{wi}^* = \begin{cases} V + y_i V & (V \geq \delta), \\ V + y_i \delta & (V < \delta), \end{cases} \tag{30}$$

where δ is minute constant value. At vehicle start ($V = 0$), the vehicle velocity is assumed to be constant value δ in the range of $V < \delta$ to avoid the wheel velocity reference to be always zero.

B. Optimum driving force reference

In this subsection, the optimum driving force distribution control system is explained. The driving force references for front and rear wheel fulfilled the optimum driving distribution ratio is generated. These references are given by feedforward.

$$F_{df} = \Big(\frac{l_r}{l} - \frac{h_g}{lg}a_x\Big)F_{ref} \tag{31}$$

$$F_{dr} = \Big(\frac{l_f}{l} + \frac{h_g}{lg}a_x\Big)F_{ref} \tag{32}$$

The system of optimum driving force distribution control is shown in Fig. 7. In (31), (32), the cofficient of vehicle driving force reference F_{ref} are equivalent to $1 - k_{opt}$ and k_{opt} in Fig. 7.

C. Driving force observer

In this subsection, the driving force observer is explained. From (1), the driving force observer is designed from the information of the motor torque and the wheel velocity. The system of driving force observer is shown in Fig. 8. In Fig. 8, real value of the wheel inertia is taken as the nominal value of wheel inertia. The motor torque reference is used as the information of the motor torque since the system of motor torque can follow the reference immediately. The wheel velocity sensor is used for mesuring the wheel velocity.

D. Wheel velocity control

In this subsection, the system of wheel velocity control which is the inner loop of the system of driving force control in Fig. 7 is explained. In this peper, massive driving force is caused on tire, so that it is necessary to consider an influence of driving force to the nominal plant of wheel. By differentiating (6) with respect to the time and substituting (1), (2), and (3), the following equation is obtained.

$$\dot{\omega_i} = \frac{T_i + r^2 M \omega_i \dot{\lambda_i}}{r^2 M(1-\lambda_i) + J_{wi}} \tag{33}$$

From (33), the nominal plant of wheel control that ignored $\dot{\lambda}$ is obtained.

$$\frac{\omega_i}{T_i} = \frac{1}{(r^2 M(1-\lambda_n) + J_{wi})s}, \tag{34}$$

where λ_n is the nominal slip ratio for the driving force. PI controller which is designed by pole assignment is implemented.

E. Driving force control

In this subsection, the system of driving force control in Fig. 7 is explained. The nominal plant of driving force is represented by

$$\frac{F_{di}}{\lambda_i} = D_{si}. \tag{35}$$

PI controller which is designed by pole assignment is implemented. The transfer function from the reference to the driving force is represented by

$$\frac{F_{di}}{F_{di}^*} = \frac{K_P D_{si} s + K_I D_{si}}{(1 + K_P D_{si})s + K_I D_{si}}, \tag{36}$$

where K_P is proportional gain, K_I is integral gain.

VI. Simulation

In this section, the simulation was performed to confirm the loss reduction for optimum driving force distribution control. In the simulation, the vehicle specifications, shown in the Table. I, are used. The vehicle model considering a variation of normal force shown in Fig. 5 is used. The reference of driving force was set for vehicle acceleration to be a_x=1.0 [m/s^2]. The poles both of driving force controller and wheel velocity controller was set to -4.3 [rad/s] and -20 [rad/s], respectively. The time response of optimum driving distribution is shown in Fig. 9. In Fig. 9(a), massive driving force at vehicle start was generated momentarily because a minute constant δ is used instead of the information of wheel velocity. The slip ratios in front and rear wheel is the same as results shown in Fig. 9(b). The time response of motor torque is similar to the response of driving force as shown in Fig. 9(c). The motor torque is dominated by driving force when the wheel is adhesive. The wheel velocity in front and rear is the same as shown in Fig. 9(d) because these slip ratios is the same. From these results, the motor output is shown in Fig. 9(e).

In order to evaluate the loss reduction, the motor output or the energy fulfilled the optimum distribution ratio is compared with driving force that filled only in front wheel ($k_f = 0$) or rear wheel ($k_f = 1.0$). The remarkable difference is not easy to confirm the loss reduction in the motor output. Therefore, the energy which is a integration value of the motor output, is compared with these distribution ratio in a certain speed region. The simulation result is shown in Table. II. From Table. II, it is confirmed that the energy loss is mimimum in the optimum distribution ratio. In a speed region of 10-30 [km/h], the difference of the energy betweern optimum distribution ratio and front only reference ($k_f = 0$), or rear only reference ($k_f = 1.0$) are about 360 [Ws], 120 [Ws]. Furthermore, the motor output in a high-speed region can be decreased in Table. II.

VII. Experiment

In this section, the experiment results are shown. The experiment is performed on the high friction road. The time response of optimum diving force distribution control is shown in Fig. 10. The response of driving force has overshoot since a minute constant value δ is used instead of the information of wheel velocity at vehicle start.

TABLE II
Simulation Result

Drive System	RECS	Front Drive	Rear Drive
Range	Energy[kWs]	Energy[kWs]	Energy[kWs]
10-30[km/h]	29.70	30.06	29.82
10-100[km/h]	367.4	371.8	369.0

The experiment of acceleration was done to verify the loss reduction for given optimum distribution ratio. The vehicle acceleration is set to be $a_x = 1.0$ [m/s^2]. It is difficult to measure precise motor output when the vehicle running. Therefore, the loss evaluation is performed indirectly by measuring the input power of inverters. The electric loss of inverter and motor is ignored in the evaluation. The evaluation equation is represented by

$$V_{dc} I_{dc} = V_{dc}(I_{dcf} + I_{dcr}), \tag{37}$$

where V_{dc} is the dc-bus voltage of inverters, I_{dcf}, I_{dcr} is the current that flows to inverters for front and rear wheels. The energy loss is measured five times. Table. III and Fig. 11 shows each averages of that experiment results and the error bar. The energy loss for optimum driving force ratio is minimum. Meanwhile, the superiority of results distributed only to front wheel and rear wheel have reversed. This is why that the loss of the motor and inverter are included in the result.

TABLE III
Experimental Result

Drive System	RECS	Front Drive	Rear Drive
Range	Energy[kWs]	Energy[kWs]	Energy[kWs]
10-30[km/h]	61.00	62.27	75.36

VIII. Conclusion

In this paper, a range extension control system based on load transfer is proposed. The effectiveness of the proposed method was verified by the simulation and the experiment. Meanwhile, the superiority between front only reference ($k_f = 0$) and rear only reference ($k_f = 1.0$) differ from the simulation. This problem could be due to the electric loss and the mechanical loss.

The future work will be the precise evaluation of the motor output. Furthermore, the novel proposal of range extension control system considering the efficiency of motor, chopper, or inverter, should be studied.

Acknowledgment

Finally, this research was partly supported by Industrial Technology Research Grant Program from New Energy and Industrial Technology Development Organization (NEDO) of Japan and in part by the Ministry of Education, Culture, Sports, Science and Technology grant number 22246057.

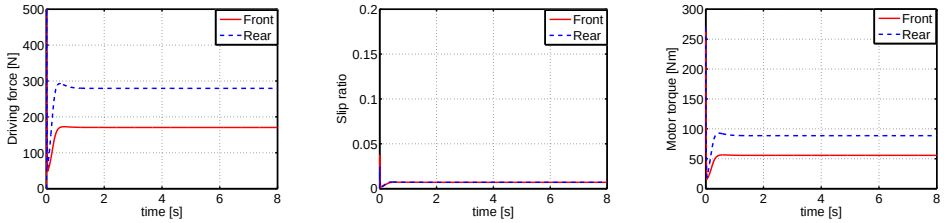

(a) Driving force (b) Slip ratio (c) Motor torque

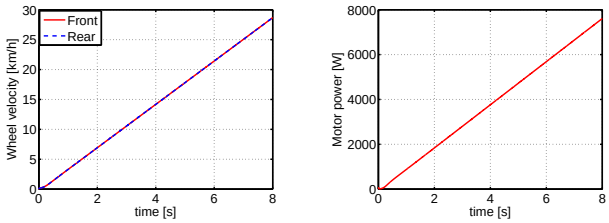

(d) Wheel velocity (e) Motor output

Fig. 9. Simulations - Optimal Driving Force Distribution Control

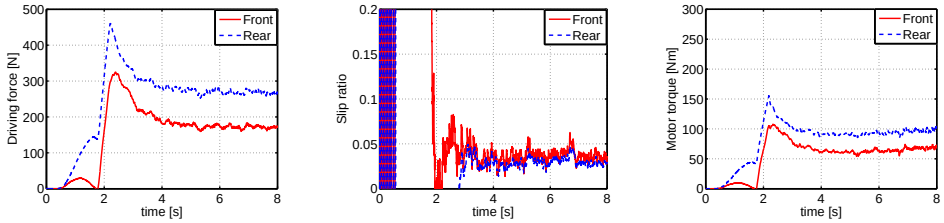

(a) Driving force (b) Slip ratio (c) Motor torque

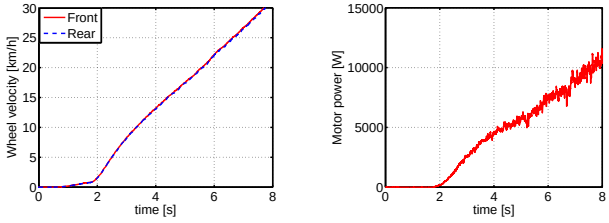

(d) Wheel velocity (e) Motor output

Fig. 10. Experimental Results - Optimal Driving Force Distribution Control

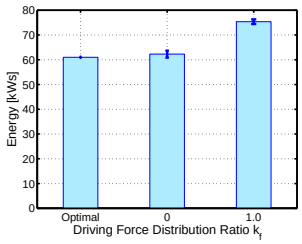

Fig. 11. Experimental Result

REFERENCES

[1] Y.Hori: “Future Vehicle by Electricity and Control-Reserch on Four-Wheel-Motored: UOT Electric March II”, IEEE Trans. IE, Vol.51, No.5, 2004

[2] H.Sado, S.Sakai, and Y. Hori: “Road Condition Estimation for Traction Control in Electric Vehicle”, In Proc. 1999 IEEE InternationalSymposium on Industrial Electronics, pp.973-978, 1999

[3] K.Fuji and H.Fujimoto: “Traction Control based on Slip Ratio Estimation Without Detecting Vehicle Speed for Electric Vehicle”, in Proc. The Fourth Power Conversion Conference, Nagoya, pp.688-693, 2007

[4] M.Yoshimura, H.Fujimoto: “Driving torque control method for electric vehicle with in-wheel motors”, IEEJ Trans. on Industry Applications, Vol.131, No.5, pp.1-8, 2010 (in Japanese)

[5] H.Sumiya, H.Fujimoto: “Range Extension Control System for Electric Vehicle with Active Front Steering and Driving/Braking Force Distribution on Curving Road”, in Proc. 36th Annual Conference of the IEEE Industrial Electronics Society, Arizona, pp.2346-2351, 2010

[6] T.Suzuki, H.Fujimoto: “Proposal of Range Extension Control System by Drive and Regeneration Distribution Based on Efficiency Characteristic of Motors for Electric Vehicle”, IEEJ Techinical Meeting Record, IIC-10-019, 2010 (in Japanese)

[7] H. B. Pacejka, and E.Bakker: “The Magic Formula Tyre Model”, Tyre model for vehicle dynamic analysis:proceeding of the1st International Colloquium on Tyre Models for Vehicle Dynamics Analysis, held in Delft, The Netherlands, 1991